This paper describes objective technical results and analysis. Any subjective views or opinions that might be expressed in the paper do not necessarily represent the views of the U.S. Department of Energy or the United States Government.

Sub Topic: Diagnostics

SAND2019-10537C

2019 WSSCI Fall Technical Meeting
Organized by the Western States Section of the Combustion Institute
October 14–15, 2019
Albuquerque, New Mexico

Emissivity Measurements of YAG:Dy and MgFGeO:Mn

Wendy Flores-Brito[1,2], Peter Vorobieff[1], Jacob T. Mahaffey[2], Andrew Vackel[2], Kathryn N. G. Hoffmeister[2,]*

[1]Department of Mechanical Engineering University of New Mexico, Albuquerque, New Mexico, United States
[2]Sandia National Laboratories, Albuquerque, New Mexico, United States
[*]Corresponding Author Email: kngabet@sandia.gov

Abstract: Emissivity is defined as the ratio of a material's thermal radiation emission, compared to a perfect emitter or black body (ε=1), at the same temperature and wavelength all under the same viewing conditions. However, emissivity can change depending on the processes to which the material has been subjected to. Thermographic phosphors (TP) are ceramic based phosphorescent materials that have a temperature dependent emission. The focus of this work is to study and measure the thermal radiation emissivity of Dysprosium doped Yttrium Aluminum-Garnate (YAG:Dy) and Manganese doped Magnesium Fluoro-Germanate (MgFGeO:Mn). Tests were conducted on both an Aerosol Deposited or AD (room temperature coating method that plastically deforms and bonds the particles onto the surface) and a "painted-on" (powder mixed with alcohol and brushed on the substrate) stainless steel sample. A Sandia LED driver, with a UV LED (365nm), was used as the light source to illuminate the samples inside a Watlow heater. These samples were submitted to a temperature range of 50-550°C at approximately 50°C steps; the data was collected utilizing a FLIR A655 camera. The YAG:Dy temperature vs. emissivity curve is fairly stable. On the other hand, for the MgFGeO:Mn, the emissivity decreases with temperature. For both AD samples, compared to the "painted-on" samples, a decrease in emissivity is shown. This could be as a result of the difference in thickness between the two coatings or the plastic deformation the particles undergo during the AD.
Keywords: Thermographic Phosphors, Emissivity, Aerosol Deposition, IR Camera

1. Introduction

Temperature is one of the most important parameters used to monitor and/or model an experiment. Thermometry, or the process of measuring temperature, can be divided into three main groups: intrusive, non-intrusive and semi-intrusive. Depending on the type of application any one or a combination of these can be used. For the case of high temperature and high voltage environments (such as combustion), the reliability of intrusive methods, like thermocouples (TC), becomes questionable. During testing, the TCs can detach from the test unit, act as a heat sink or suffer from Seebeck effects. Remote thermometry, such as phosphor or IR thermometry, can be used as an alternative to monitor temperature. But, just as with the use of thermocouples, there are sources of error when using remote thermometry as well as during modeling thermal radiation effects. One of the largest sources of errors in both circumstances is a material's changing emissivity.

Sandia National Laboratories is a multimission laboratory managed and operated by National Technology & Engineering Solutions of Sandia, LLC, a wholly owned subsidiary of Honeywell International Inc., for the U.S. Department of Energy's National Nuclear Security Administration under contract DE-NA0003525.

Sub Topic: Diagnostics

Infrared (IR) Thermometry:

All forms of matter emit radiation [1]. The amount of thermal radiation emitted by an opaque surface was first determined experimentally by Stefan in 1879 to be:

$$E = \varepsilon\sigma T^4 \quad (1)$$

Where E is the emissive power, ε is the emissivity (equal to one if it is a perfect black body), σ is the Stefan-Boltzmann constant (5.6697×10^{-8} W/m^2*K^4), and T is the absolute temperature [1].

The subsequent transport of this emitted radiation does not require the presence of any matter and it's believed to travel as either a collection of photons or electromagnetic waves [1]. Thermal radiation energy is typically emitted in the infrared range; therefore, IR cameras are used to capture these emissions and correlate them to the object's temperature.

No Infrared camera reads temperature directly. They read IR energy coming from the target which includes emitted, reflected and sometimes transmitted IR energy [2]. In formulating an energy balance on the surface, the following equation must be considered:

$$1 = \alpha + \rho + \tau \quad (2)$$

Where α is absorbed energy, ρ is the reflected energy, and τ is the transmitted energy. Today's cameras correct for emissivity only for opaque targets whose transmittivity is zero [2]; which is the typical case in most engineering applications [2]. In these cases, equation (2) becomes:

$$1 = \rho + \alpha \quad (3)$$

If Kirchhoff's Law of Thermal Radiation is also assumed [3], then the absorptivity is equal to the emissivity and a relation between reflectivity and emissivity can be determined:

$$1 = \rho + \varepsilon \quad (4)$$

Emissivity can be defined as a ratio between a material's thermal radiation emission and that of a perfect black body (ε=1), at the same temperature and wavelength. It ranges from 0 to 1 and can vary depending on the material, surface finish, geometry, view angle and temperature. IR cameras have these equations incorporated to their system, but if the emissivity is not known, the temperature reading is not correct.

Phosphor Thermometry:

Laser diagnostics technique used for surface temperature measurements. It is often used to measure temperature in combustion environments due to its insensitivity to scattered light, e.g. chemiluminescence from combustion soot [4-11]. Exploits the temperature-dependent luminescence of thermographic phosphors or TP (ceramic based powders doped with different elements, typically rare earth metals). After the TP is excited with a light source, i.e. Laser or LED, the emission at the temperature dependent wavelength is collected and either the time or intensity dependence is analyzed [10]. For the intensity ratio method, each thermographic phosphor has a peak at a certain wavelength, which increases with temperature, and a constant intensity at another wavelength [10]. Taking data simultaneously at both wavelengths, a ratio (which increases with temperature) between the two signals can be used to determine the temperature. The lifetime decay method computes the luminescence duration of the phosphor after excitation, which exponentially shortens as temperature rises.

Due to the high sintering temperature of ceramics, which typically requires a plasma spray or chemical/vapor deposition. These types of bonding techniques may put stress or added heat on the samples, which aren't desired on certain temperature sensitive applications. A room temperature bonding technique that retains the temperature dependent properties of the TP is the Aerosol Deposition (AD) [12].

Aerosol Deposition:

Aerosol Deposition was initially intended as an alternative way to create ceramic-coated materials without the need of high sintering temperatures. This would broaden the range of applications, allowing ceramics to be bonded with materials that have lower melting points. Some of the applications and components on which Aerosol Deposition has been successfully tested include: aluminum, piezoelectric materials, titanium dioxide, biocomponents, magnetic materials, fuel cells, sensing materials, and batteries [13-16].

Aerosol Deposition is a new, room temperature coating technique which requires no input thermal energy, no binders, and only uses the kinetic energy (supersonic velocities) of the particles to produce highly dense coatings. The Aerosol Deposition process uses nano-to-micron-sized feedstock particles, which are accelerated to supersonic velocities to create metallic, ceramic, and carbide coatings [16, 17]. The carrier gas usually consists of N_2 or He and transports dry particles of the desired material to a nozzle, where they are accelerated into a vacuum chamber. The supersonic particles impinge on the surface of the substrate and plastically deform (ceramics included), resulting in a strong mechanical bond between the substrate and coating material [16-19]. Each subsequent collision tamps the surface to produce a highly dense, void-free, adherent coating, capable of large thickness (up to 10s of microns). The shock involved during collisions results in fragmentation of the particles and produces grain sizes on the order of 10s of nanometers (ideal for inexpensive polycrystalline laser materials). A schematic of the Aerosol Deposition facility used in this study and a diagram of the spray process are given in Figure 2. For this study, testing with micron particles of YAG:Dy and MgFGeO:Mn was performed. Previous results to compare the temperature dependent properties of a baseline sample and Aerosol Deposited YAG:Dy are shown in the graph in Figure 1 [12].

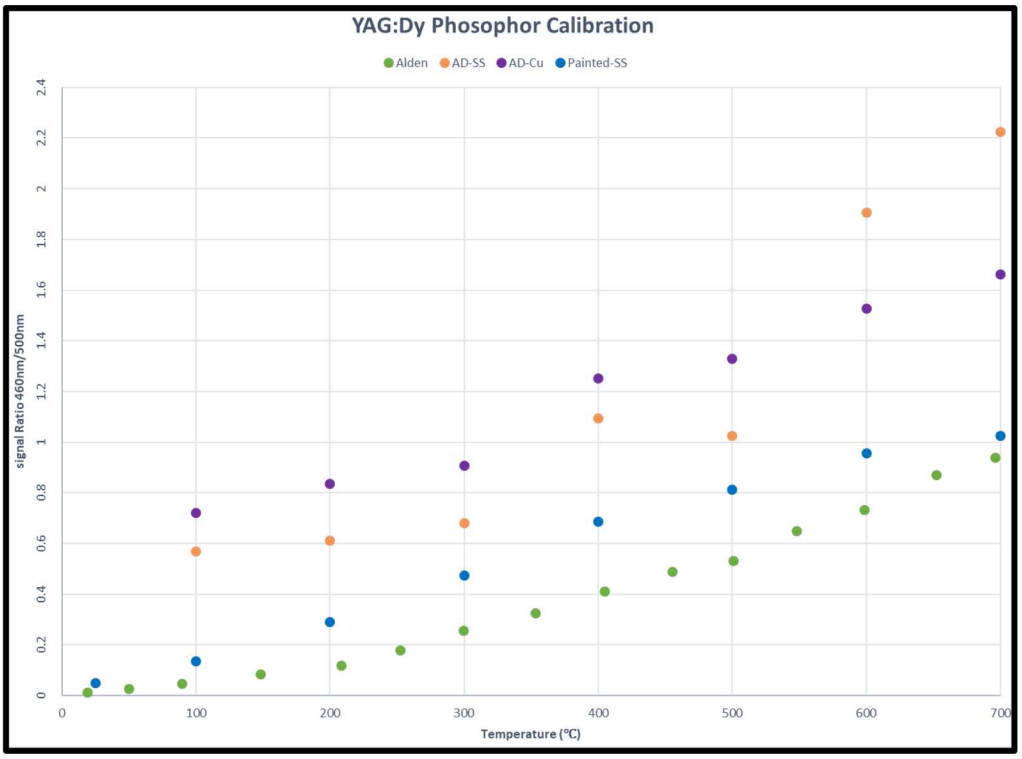

Figure 1. YAG:Dy Calibration curves (*Alden* paper, Aerosol Deposition stainless steel and copper sample and "painted-on" sample) [12].

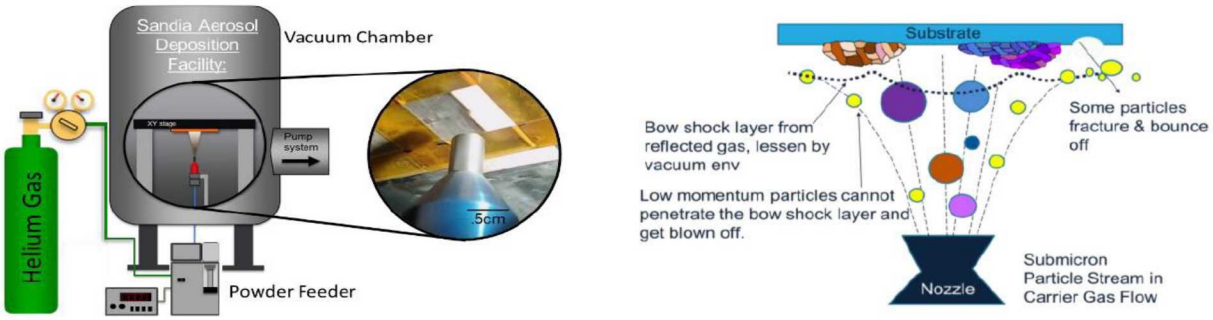

Figure 2. Sample schematic of Aerosol deposition coating process [12].

2. Methods / Experimental

For this study two different thermographic phosphors, Yttrium Aluminum-Garnate doped with Dysprosium (YAG:Dy) and Manganese doped Magnesium Fluoro-Germanate (MgFGeO:Mn), and coating methods are used and compared. One sample of each was made with each coating technique (Aerosol Deposition and "painted-on") for a total of four samples. Five tests were conducted with each sample, heating them from 50°C to 550°C in 50°C intervals; data sets of 100 images were taken at each temperature. Small ROIs (10x10 pixels) in various parts of the sample were analyzed during the post processing to obtain temperature versus emissivity plots.

Samples:

Four stainless steel substrates were coated with thermographic phosphors. Two were coated using the Aerosol Deposition method (one with YAG:Dy and the other with MgFGeO:Mn). The other two samples were prepared by mixing the TP with alcohol and "painted-on" the sample using a regular paint brush. Thermocouples were also attached to the samples to verify at what temperature the samples were during the experiment. Figure 3 shows the four stainless steel samples (two YAG:Dy and two MgFGeO:Mn) used for experimental purposes. The AD samples (top and bottom left images) have taken a darker color after the bonding process; compared to the typical white or lighter color of these specific phosphors (samples on the right images).

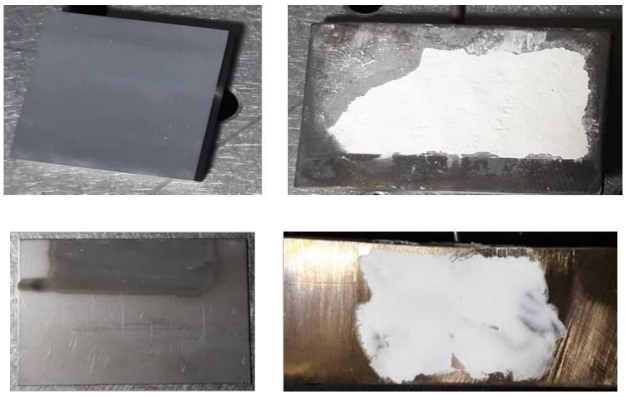

Figure 3. Stainless steel samples. (Top left) Aerosol Deposited YAG:DY. (Top right) "Painted-on" YAG:DY. (Bottom left) Aerosol Deposited MgFGeO:Mn. (Bottom right) "Painted-on" MgFGeO:Mn.

Experimental Setup and Procedure:

The samples are placed inside a 120V Watlow heater (Figure 4.C) where they are subjected to an increasing temperature range of 50-550°C in increments of 50°C steps. The heater was controlled using a FLUKE 725 multifunction process calibrator; which also was used to read the thermocouple temperature. A Sandia LED Driver [20] with a 365nm UV LED (Figure 4.B) was used to illuminate the samples during testing. The driver is powered using a BK Precision Power Supply and controlled with a Stanford Delay Generator. Data collection was done using a FLIR A655sc camera (Figure 4.A), controlled with the research IR computer program.

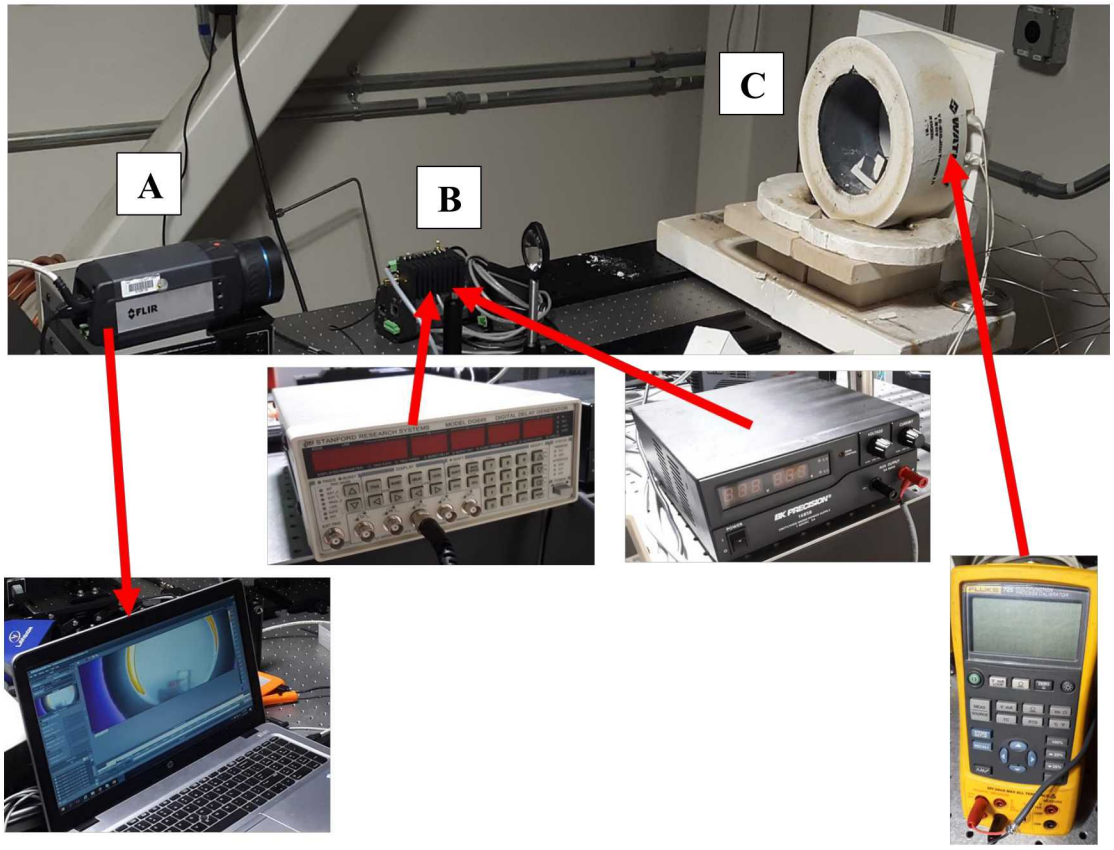

Figure 4. Experimental Setup

Calibration and Post Processing:

Infrared cameras are calibrated using a black body or some sort of material that has a known emissivity. The object is heated in the same manner as the test samples and the data at each temperature is recorded. Figure 5 shows a typical Temperature versus camera intensity/digital level calibration curve that can be used in combination with equation (5) to obtain the material's emissivity at a certain temperature [2]. A MATLAB code incorporating equation (5) backtracks the sample's emissivity.

$$\varepsilon_t = \frac{I_{mt} - I_{mb}}{I_{Rt} - I_{mb}} \tag{5}$$

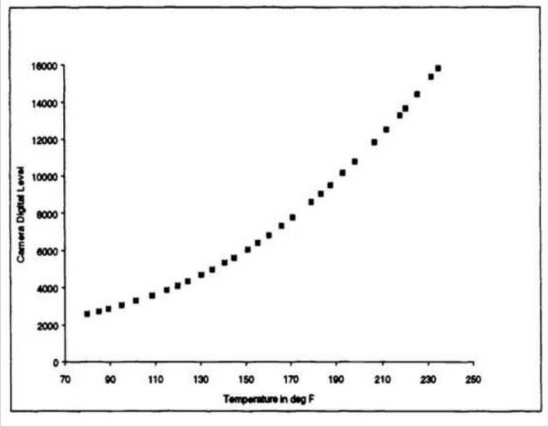

Figure 5. Typical IR camera temperature versus intensity calibration curve [2].

3. Results and Discussion

Equation (1) for thermal radiation is in terms of temperature, emissivity and a constant. This means that if the temperature changes, for the actual thermal radiation to be correct, the other non-constant term also must change. Figure 6 displays the thermocouple temperature (black solid line) versus the temperature read by the IR camera (dashed lines, red for the "painted-on" samples and blue for AD sample) at a constant emissivity. As the temperature increases, the difference between the two readings also increases. To compensate for this difference in the IR camera's reading, the emissivity has to be corrected; which means there is a change in the emissivity of the samples.
After processing the collected data for all four samples, temperature versus emissivity plots are generated (Figures 7 & 8). Figure 7 is for YAG:Dy and Figure 8 plots the MgFGeO:Mn curves. Both YAG:Dy samples have fairly stable emissivities; on the other hand, for the MgFGeO:Mn the emissivity decreases with temperature. In both phosphor cases the AD samples (blue lines) have a lower emissivity than the "painted-on" samples. This difference is still being looked into, but it is thought to be due to the difference in thickness or the surface finish.

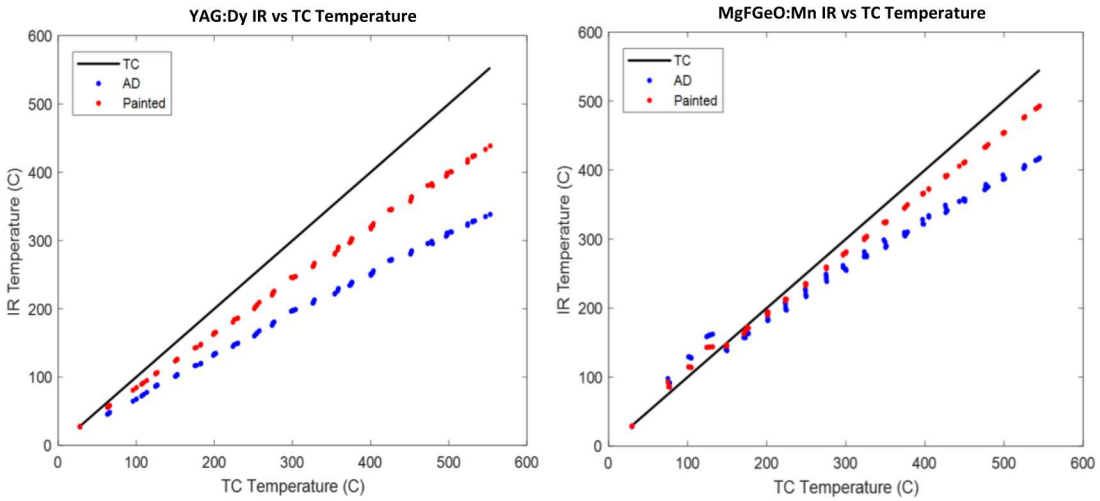

Figure 6. Thermocouple versus IR camera temperature. (Left) YAG:Dy. (Right) MgFGeO:Mn.

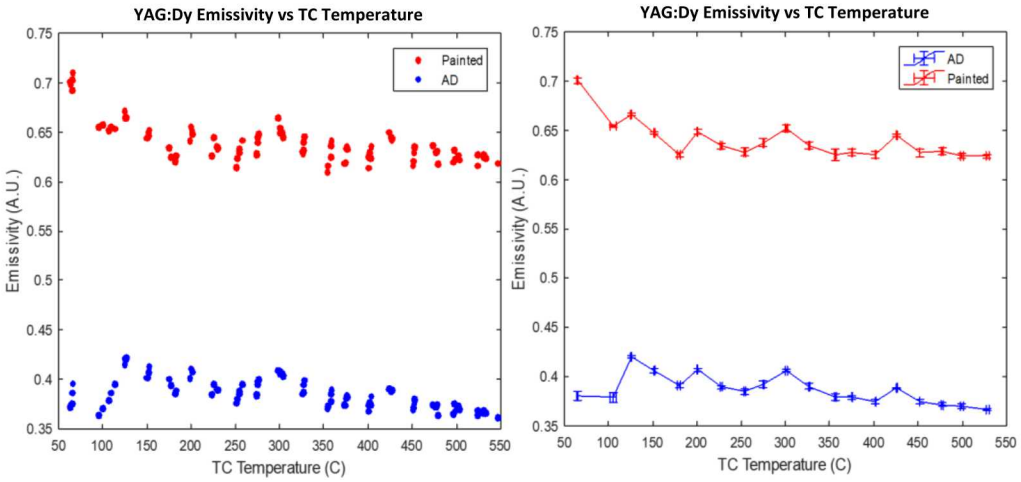

Figure 7. Emissivity versus temperature curves for YAG:Dy. (Left) Results per test. (Right) average results of all tests.

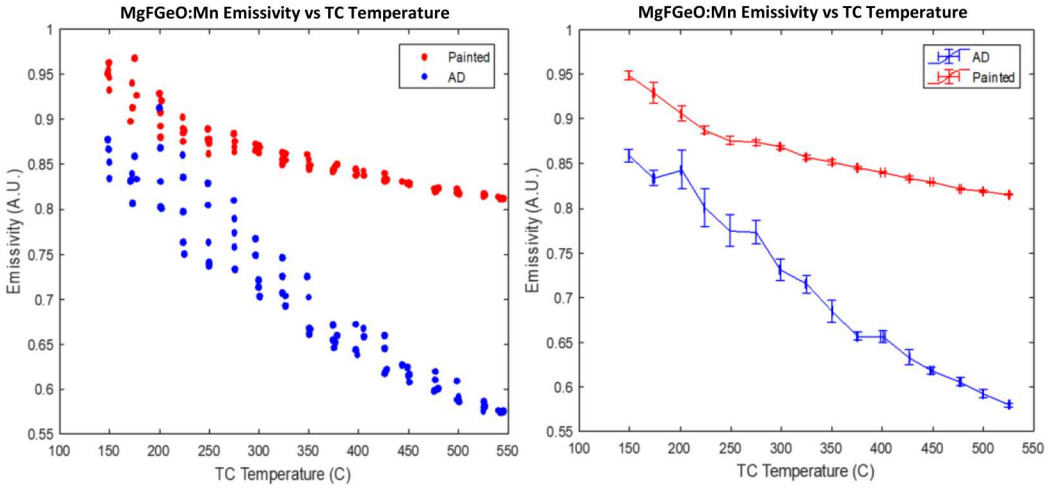

Figure 8. Emissivity versus temperature curves for MgFGeO:Mn. (Left) Results per test. (Right) average results of all tests.

4. Conclusions

The veracity and accuracy of thermal radiation modeling and experimental data is highly dependent on knowing the correct emissivity in varying environments. In the case of thermographic phosphors within the temperature range studied in this experiment, there is a similarity between the curves for the two different coating techniques and samples for each phosphor. Even though more tests are needed, this could mean that thermographic phosphor's can be calibrated to be used as a reference point when doing IR thermometry. The Aerosol deposition process has an effect in the thermographic phosphor's emissivity that is believed to be due to thickness or surface finish differences that is still being researched. More tests will be conducted using different cameras, TP coating thicknesses, a larger temperature range, varying heater ramp rates, and test the actual applicability of utilizing thermographic phosphors for simultaneous temperature measurement and IR reference point.

5. Acknowledgements

Sandia National Laboratories is a multimission laboratory managed and operated by National Technology & Engineering Solutions of Sandia, LLC, a wholly owned subsidiary of Honeywell International Inc., for the U.S. Department of Energy's National Nuclear Security Administration under contract DE-NA0003525. The authors would also like to thank Vincent Valdez, Michael Montoya and Daniel Roybal for their help in the lab during testing.

6. References

[1] F.P. Incropera, D.P. Dewitt, T. L. Bergman, A.S Lavine, Introduction to Heat Transfer, 5th Edition, John Wiley & Sons, Inc., USA, 2007.

[2] R.P. Madding, Thermosense XXI (1999), doi:10.1117/12.342307.

[3] D.A. Kaminski, M.K. Jensen, Introduction to Thermal and Fluid Engineering, John Wiley & Sons, Inc., USA, 2005.

[4] A. Khalid, K. Kontis, Thermographic Phosphors for High Temperature Measurements: Principles, Current State of the Art and Recent Applications, Sensors (2008) 8, pp. 5673–744, doi:10.3390/s8095673.

[5] M. Yu, G. Särner, C.C.M. Luijten, M. Richter, M. Aldén, R.S.G. Baert, et al, Survivability of thermographic phosphors (YAG:Dy) in a combustion environment, Measurement Science and Technology (2010) 21:037002, doi:10.1088/0957-0233/21/3/037002.

[6] J.I. Eldridge, S.W. Allison, T.P. Jenkins, S.L. Gollub, C.A. Hall, D.G. Walker, Surface temperature measurements from a stator vane doublet in a turbine afterburner flame using a YAG:Tm thermographic phosphor, Measurement Science and Technology (2016) 27:125205, doi:10.1088/0957-0233/27/12/125205.

[7] A. Omrane, F. Ossler, M. Aldén, Temperature measurements of combustible and non-combustible surfaces using laser induced phosphorescence, Experimental Thermal and Fluid Science (2004) 28, pp. 669–76, doi:10.1016/j.expthermflusci.2003.12.003.

[8] A.C. Eckbreth, Laser Diagnostics for Temperature and Species in Unsteady Combustion, Unsteady Combustion (1996) pp. 393–410, doi:10.1007/978-94-009-1620-3_18.

[9] A. Omrane, Y. Wang, U. Göransson, G. Holmstedt, M. Aldén, Intumescent coating surface temperature measurement in a cone calorimeter using laser-induced phosphorescence, Fire Safety Journal (2007) 42, pp. 68–74, doi:10.1016/j.firesaf.2006.08.006.

[10] M. Aldén, A. Omrane, M. Richter, G. Särner, Thermographic phosphors for thermometry: A survey of combustion applications, Progress in Energy and Combustion Science (2011) 37, pp. 422–61, doi:10.1016/j.pecs.2010.07.001.

[11] J. Brübach, C. Pflitsch, A. Dreizler, B. Atakan, On surface temperature measurements with thermographic phosphors: A review, Progress in Energy and Combustion Science (2013) 39, pp. 37–60, doi:10.1016/j.pecs.2012.06.001.

[12] W. Flores-Brito, J. Mahaffey, A. Vackel, K.N.G. Hoffmeister, Aerosol Deposition of Dysprosium-Doped Yttrium-Aluminum-Garnet for Phosphor Thermography Applications, AIAA Scitech 2019 Forum (2019) doi:10.2514/6.2019-2102.

[13] D. Hanft, J. Exner, M. Schubert, T. Stöcker, P. Fujerer, R. Moos, An Overview of the Aerosol Deposition Method: Process Fundamentals and New Trends in Materials Applications, Journal of Ceramic Science and Technology (2015) 06, pp. 147–82. doi:10.4416/JCST2015-00018.

[14] J. Akedo, J. Ryu, D.Y. Jeong, S. Johnson, Aerosol Deposition (AD) and Its Applications for Piezoelectric Devices, Advanced Piezoelectric Materials (2017) pp. 575–614, doi:10.1016/b978-0-08-102135-4.00015-1.

[15] P. Sarobol, M. Chandross, J.D. Carroll, W.M. Mook, D.C. Bufford, P.G. Kotula, B.B. McKenzie, B.L. Boyce, K. Hattar, A.C. Hall, Room Temperature Solid-State Deposition of Alumina., Glenn T. Seaborg - Contributions to Advancing Science, (2014) Available: https://www.osti.gov/servlets/purl/1242755.

[16] J. Akedo, Aerosol Deposition of Ceramic Thick Films at Room Temperature: Densification Mechanism of Ceramic Layers, Journal of the American Ceramic Society (2006) 89, pp. 1834–1839, doi:10.1111/j.1551-2916.2006.01030.x.

[17] J. Akedo, M. Lebedev, Ceramics Coating Technology based on Impact Adhesion Phenomenon with Ultrafine Particles—Aerosol Deposition Method for High Speed Coating at Low Temperature, Materia (2002) pp. 459–466.

[18] P. Sarobol, M. Chandross, J.D. Carroll, W.M. Mook, D.C. Bufford, B.L. Boyce, et al, Room Temperature Deformation Mechanisms of Alumina Particles Observed from In Situ Micro-compression and Atomistic Simulations, Journal of Thermal Spray Technology (2015) 25, pp. 82–93, doi:10.1007/s11666-015-0295-2.

[19] E. Calvié, L. Joly-Pottuz, C. Esnouf, P. Clément, V. Garnier, J. Chevalier, et al, Real time TEM observation of alumina ceramic nano-particles during compression, Journal of the European Ceramic Society (2012) 32, pp. 2067–71. doi:10.1016/j.jeurceramsoc.2012.02.029.

[20] E. Westphal, W. Flores-Brito, B.R. Wilburn, K.N.G. Hoffmeister, Study of Sensitivity vs. Excitation Time of LED Excited Thermographic Phosphors, AIAA Scitech 2019 Forum (2019) doi:10.2514/6.2019-2106.